

Mutual amplification of sensory nerve outgrowth and tumor progression in myeloma

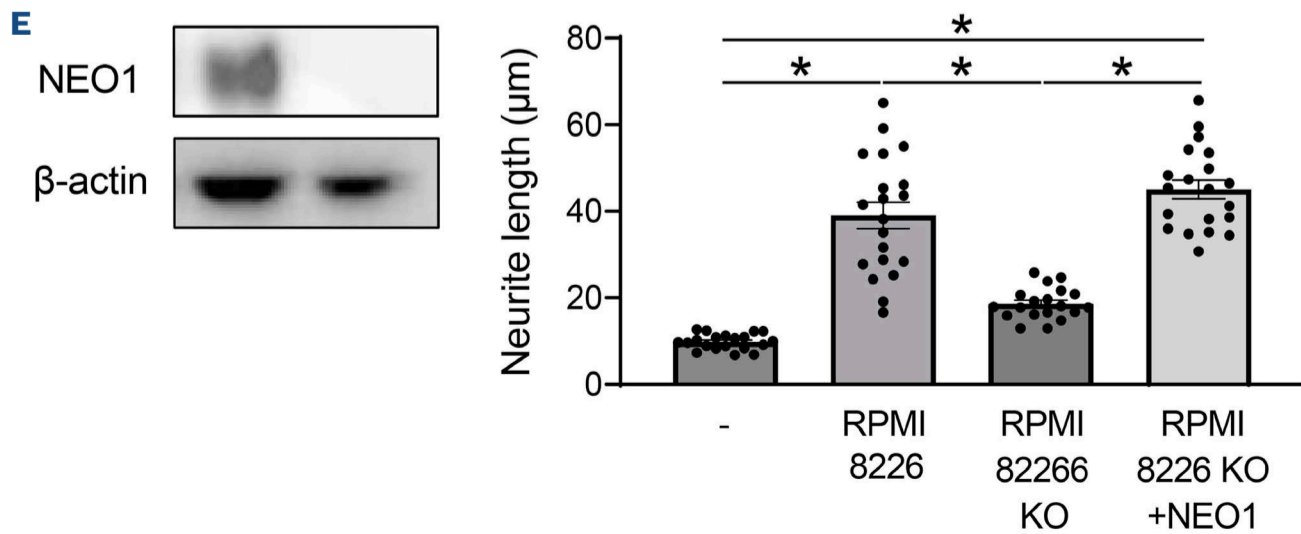
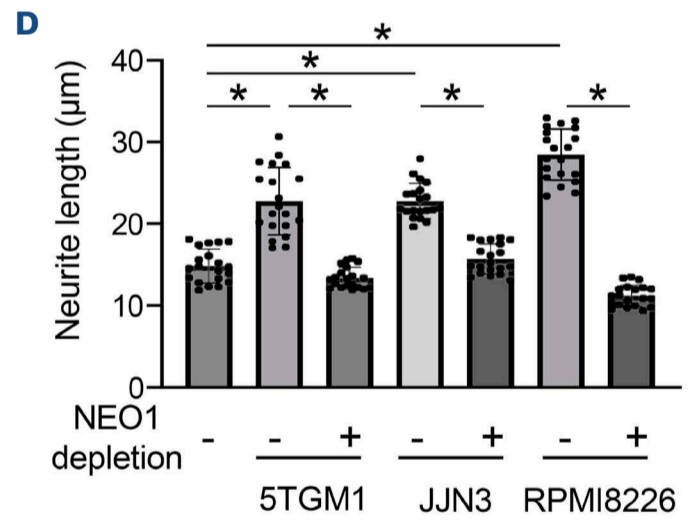
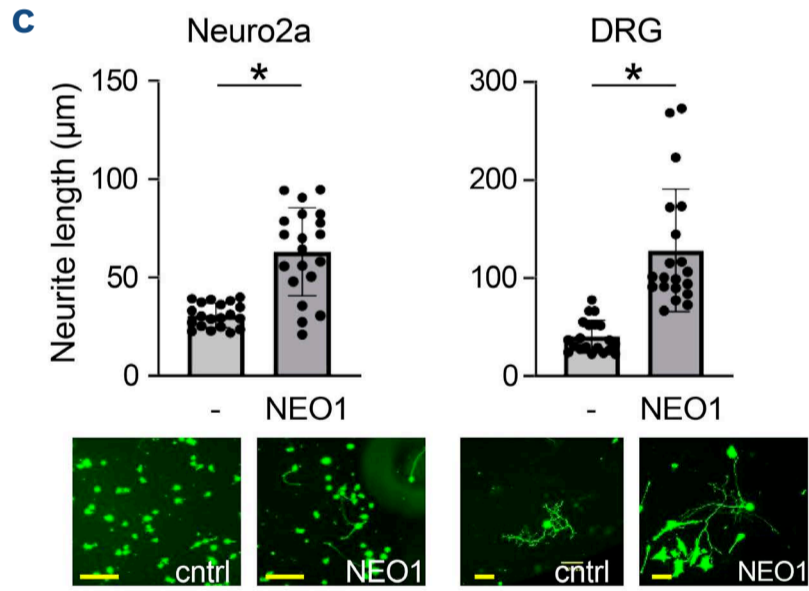
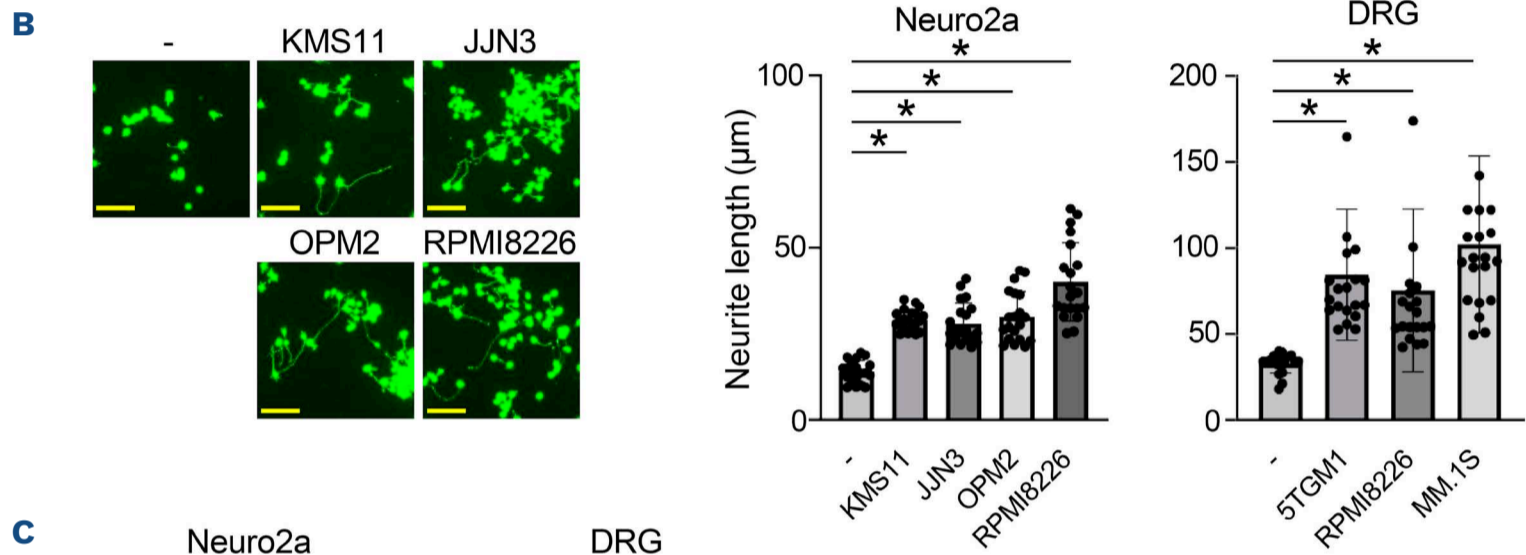
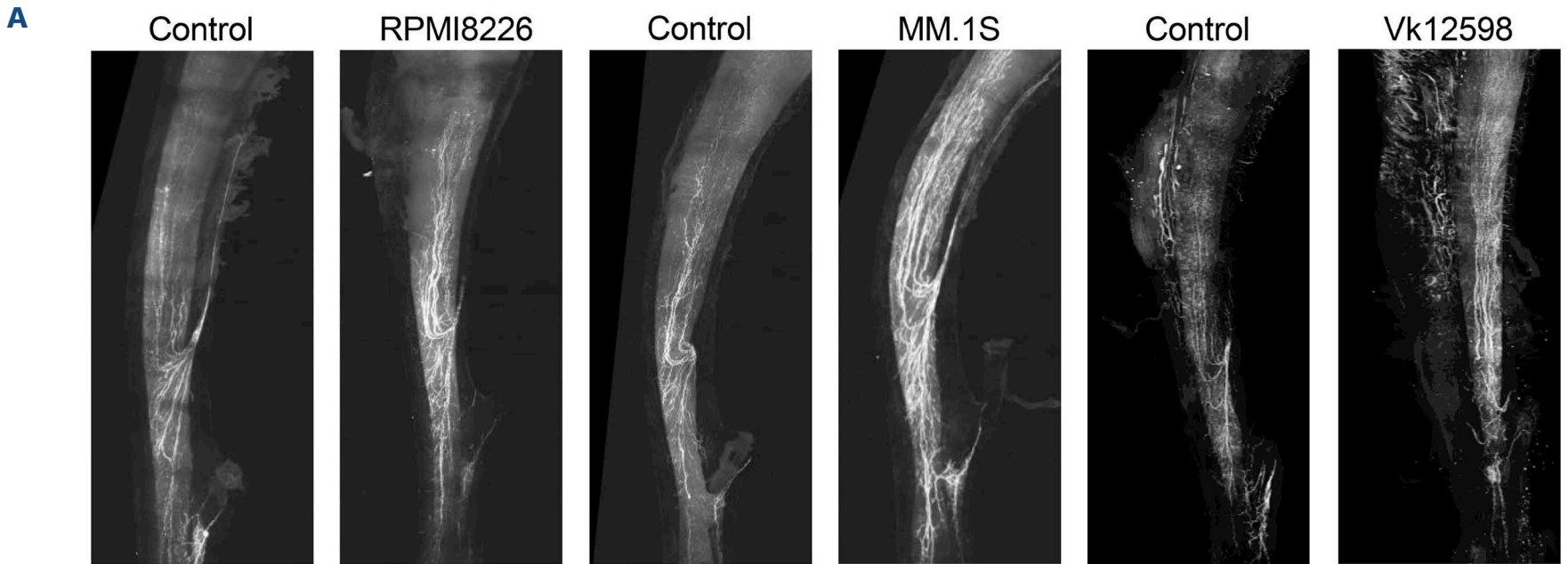
Multiple myeloma (MM) is characterized by preferential accumulation of tumor cells in the bone marrow with devastating bone destruction. Bone pain is a common and debilitating complication associated with osteoclastic bone destruction in MM and cancer metastasis to bone. Excitation and sensitization of sensory nerves (SN) evoke pain. Calcitonin gene-related peptide (CGRP)-positive SN have been reported to increase and intermingle with MM cells in bone marrow in mouse MM models.¹ SN extend their neurites in acidic conditions in MM bone marrow lesions in mouse MM models with SN excitation as shown by phosphorylation of ERK1/2 and CREB in dorsal root ganglia (DRG), suggesting an important role of acid in sprouting of SN neurites and increased susceptibility to pain.¹ Tumor innervation has been recently drawing considerable attention in growth, metastasis/invasion, and drug resistance in various cancers.^{2,3} However, little is known about SN distribution in the bone marrow and the interactions between SN and bone-residing tumors such as MM. Precise evaluation of SN distribution in the bone marrow is difficult in thin-sliced tissue specimens and requires three-dimensional SN visualization in the entire bone marrow. In the present study, we therefore aimed to three-dimensionally explore SN spreading and outgrowth in the bone marrow and clarify the underlying mechanisms of SN sprouting in MM and the role of SN in MM tumor progression. We demonstrate here that sensory innervation is increased in the bone marrow with MM lesions. Interestingly, MM cells induce SN outgrowth, which in turn promotes MM tumor progression to form a vicious cycle, posing the concept of MM progression being controlled by the peripheral nervous system.

Peripheral nerves are distributed throughout the body. In order to explore the actual state of CGRP⁺ SN distribution in the bone marrow in three dimensions, we visualized SN in bone in MM models after transparency of the entire bone by the optical clearing CUBIC method.^{4,5} The distribution and density of CGRP⁺ SN increased in the bone marrow of tibiae in different MM models implanted intra-tibially with human MM.1S and RPMI8226, and mouse Vk12598 and 5TGM1 MM cell lines, compared with control contralateral tibiae without MM tumor involvement in the same mice (Figure 1A; *Online Supplementary Figure S1A*). These results suggest that sensory innervation is enhanced in the bone marrow in MM.

To dissect the mechanisms for the SN outgrowth, we first asked if MM cells produce SN outgrowth-promoting activity. MM cell culture supernatants enhanced the neurite sprouting and outgrowth of SN derived from the neural cell line Neuro2a and primary mouse DRG cells as esti-

mated according to the previously reported investigation system⁶ (Figure 1B). We reported that TGF- β -activated kinase 1 (TAK1) plays a pivotal role in tumor progression and drug resistance along with alteration of the bone marrow microenvironment in MM, including bone metabolism and angiogenesis.⁷ Through further exploring the role of TAK1 in the microenvironmental alteration, we recently found that pretreatment on MM cells with the TAK1 inhibitor LLZ1640-2 abolished the SN neurite outgrowth promoting activity by MM cells (*Online Supplementary Figure S1B*). To elucidate MM cell-derived secreted factor(s) to promote SN neurite outgrowth, we therefore performed a comprehensive secretome analysis of MM cell lines in the presence or absence of LLZ1640-2 (*Online Supplementary Figure S2*). We selected TAK1-dependent MM cell-specific factors with high basal secretion levels (*Online Supplementary Figure S2F*), which included factors involved in the biology of the nervous system. We then screened their neurite outgrowth-promoting activity. Among the secreted MM cell-specific factors, neogenin1 (NEO1) was secreted at high basal levels from MM cells; and recombinant (r)NEO1 was found to potently enhance neurite sprouting and outgrowth in Neuro2a-derived SN in the presence of NGF and DRG cells (Figure 1C; *Online Supplementary Figure S1C*). We confirmed NEO1 secretion from primary MM cells as well as MM cell lines (*Online Supplementary Figure S1D,E*). When NEO1 was depleted from MM cell culture supernatants, their neurite outgrowth-promoting activity almost disappeared (Figure 1D; *Supplementary Figure 1D,E*). To further clarify the role of MM cell-derived NEO1, we created NEO1-knockout (KO) RPMI8226 cells. The KO cells mitigated the *in vitro* neurite outgrowth of Neuro2a-derived SN compared with control RPMI8226 cells, which was reversed by addition of rNEO1 (Figure 1E). These results suggest soluble NEO1 as a critical MM cell-derived SN neurite elongation factor.

Membrane-bound NEO1 is expressed in peripheral nerves as a receptor for neural guidance and repulsion molecules.⁸ RGM-a, a repulsive guidance molecule, is one of major NEO1 ligands which is abundantly contained in sera.^{9,10} RGM-a has been demonstrated to induce neurite retraction and axonal growth cone collapse.¹¹ rRGM-a suppressed neurite outgrowth induction by NGF (Figure 2A); however, addition of rNEO1 inhibited the rRGM-a's action (Figure 2B; *Online Supplementary Figure S3A*). rRGM-a also acutely retracted neurites when added to Neuro2a-derived SN with extended neurites (Figure 2C; *Online Supplementary Figure S3B*) and abolished actin polymerization (Figure 2D; *Online Supplementary Figure S3C*). Addition of rNEO1 almost completely inhibited the RGM-a-induced neurite retraction and actin



Continued on following page.

Figure 1. Sensory nerve neurite-outgrowth promoting activity by multiple myeloma cells. (A) Sensory nerves (SN) distribution in the bone marrow. The indicated multiple myeloma (MM) cell lines (1×10^4 cells) were inoculated into the bone marrow cavity of the tibiae of the right hind legs in SCID mice (CLEA Japan, Tokyo, Japan) (N=5 per group). Tumor-bearing tibiae (right) and intact contralateral tibiae (left, control) were resected 4 weeks after the inoculation. The samples were fixed and demineralized, and subjected to delipidation in CUBIC-L for 3 days, followed by treatment with 0.1% collagenase A for 15 minutes (min). Subsequently, the samples were incubated for 2 weeks in an antibody reaction buffer with anti-CGRP antibody diluted 1:1,000. They were post-fixed in 1% paraformaldehyde at 4°C for 1 day, and then embedded in 1% agarose gel. The embedded samples were cleared using CUBIC-R for 2 days and imaged using a light-sheet fluorescence microscope (MuVi SPIM LS&CS, Bruker Luxendo GmbH, Germany) to visualize CGRP-positive sensory nerves. Three-dimensional reconstruction of the acquired images was performed using Imaris software (version 10.2.0, Oxford Instruments KK, Tokyo, Japan). (B) Primary dorsal root ganglion (DRG) cells were isolated from C57BL/6J mice, and enzymatically dissociated in 2 mg/mL collagenase type III at 37 °C for 120 min, followed by 0.05% trypsin-EDTA at 37 °C for 10 min to obtain a single-primary DRG cell suspension. The indicated MM cell lines were cultured for 2 days at 5×10^5 /mL, and culture supernatants were harvested. The culture supernatants were added at 20% to the neural cell line Neuro2a in the presence of nerve growth factor (NGF) at 10 ng/mL and primary DRG cells. After culturing for 2 days, photos of the cells were taken after staining with calceinAM, and the length of the longest neurite from each cell was measured using NeuronJ (NIH, Bethesda, MD, USA). The representative photos of Neuro2a cells were shown (left panels). Original magnitude, $\times 100$. Size bars indicate 100 μ m. (C) Recombinant neogenin1 (NEO1) was added at 100 ng/mL to the neural cell line Neuro2a in the presence of NGF at 10 ng/mL and primary DRG cells, and after culturing for 3 days, the length of the longest neurite from each cell was measured using NeuronJ. Representative images of Neuro2a cells (original magnitude, $\times 100$) and DRG neurons ($\times 40$) are shown. Size bars indicate 100 μ m. (D) To deplete soluble NEO1, conditioned media from the indicated MM cell lines were incubated for overnight at 4°C with constant mixing with either 20 μ g/mL rabbit anti-human NEO1 antibody or normal rabbit IgG. After the incubation, protein G-agarose beads were then added and further incubated for 1 hour, followed by centrifugation at 12,000 rpm for 5 min at 4°C. The MM cell conditioned media with or without the immunodepletion of NEO1 were added at 20% to Neuro2a in the presence of NGF at 10 ng/mL. After culturing for 2 days, the length of the longest neurites from each cell were measured using NeuronJ. (E) We created *NEO1*-knockout (KO) RPMI8226 cell line in which the *NEO1* gene was knocked out with CRISPR-based gene editing. A single-guide RNA (sgRNA) targeting human *NEO1* (5'-TGACACCATCAG-GATTACGT-3') was delivered into Cas9-expressing RPMI 8226 cells via lentiviral transduction. After 48 hours of puromycin selection, single-cell-derived clones were established by limiting dilution. Loss of *NEO1* protein expression was confirmed by immunoblotting (left). The KO and control cells were cultured for 2 days at 5×10^5 /mL, and culture supernatants were harvested. The culture supernatants were added at 20% to the neural cell line Neuro2a in the presence of NGF at 10 ng/mL. rNEO1 at 100 ng/mL was added as indicated. After culturing for 2 days, the length of the longest neurite from each cell was measured using NeuronJ. Data are expressed as mean \pm standard deviation. * $P < 0.05$.

depolymerization. Therefore, soluble NEO1 from MM cells can induce neurite outgrowth at least in part through acting as a decoy receptor to inhibit RGM-a. However, rNEO1 still enhanced the neurite extension in a serum-free condition (*Online Supplementary Figure S3D*), suggesting a mechanism other than the RGM-a-mediated mechanism. NEO1 contains six fibronectin type III domains that can interact with integrin $\beta 1$ through an Arg-Gly-Asp (RGD) amino acid sequence to induce the activation of downstream signaling pathways, including the ERK/MAP kinase pathway. Soluble NEO1 can also interact with growth factors such as bone morphogenetic proteins and extracellular matrix components. These characteristic features endow soluble NEO1 with additional activities which membrane-bound NEO1 does not have.

The bone marrow microenvironment is skewed by MM cell infiltration, which is vital for MM cell growth and survival. SN outgrowth may also affect the bone marrow microenvironment in MM. Therefore, we next explored the effects of SN on MM cell growth. MM cell growth was enhanced when co-cultured with Neuro2a-derived SN or DRG cells (Figure 3A). Extracellular vesicles (EV) are recognized as crucial mediators of cellular communication in various pathological conditions including those in the nervous system and tumor microenvironment.¹² We therefore isolated EV from culture supernatants of primary DRG cells as well as Neuro2a-derived SN as previously described.¹³ The isolated EV also showed potent MM cell proliferation activity (Figure

3B). miR-21, an oncogenic microRNA, has been reported to contribute to perineural invasion and proliferation of cancers.¹⁴ As assumed, pre-treatment of DRG cells with an miR-21 inhibitor abrogated MM cell growth enhancement by DRG cell-derived EV (Figure 3C). Therefore, SN expansion in the bone marrow is suggested to promote MM cell growth at least in part through SN-secreted EV.

To further confirm the role of SN in MM tumor growth, we next examined the MM tumor progression in mice with or without pharmacological sensory denervation. Pharmacological denervation of SN was performed by subcutaneous injection of high-dose capsaicin into a lumbar dorsal region according to the previously reported method.¹⁵ Although capsaicin did not apparently affect the growth of MM cell lines *in vitro* (*data not shown*), we waited for 7 days after the last capsaicin injection to remove capsaicin from the mice and degenerate SN. SN fibers were found to be substantially decreased in the bone marrow by the pharmacological sensory denervation (Figure 3D, upper). Then, mouse 5TGM1 and human JN3 MM cells were intra-tibially inoculated. MM tumor growth was notably reduced in the mice with the sensory denervation compared to control mice (Figure 3D), suggesting a critical role of SN in MM tumor growth. Furthermore, SN spreading in the bone marrow was reduced in tibiae bearing *NEO1*-knockout (KO) RPMI8226 cells compared with those with control RPMI8226 cells (Figure 3E). IVIS images showed that tumor growth was also attenuated with the *NEO1*-KO cells, although there

was no clear difference of *in vitro* growth between the *NEO1*-KO and control cells (*Online Supplementary Figure S3E*), suggesting the critical roles of MM cell-derived *NEO1*

in neurite outgrowth of SN and MM cell growth. The present study highlights that sensory innervation is increased in the bone marrow in MM, which in turn pro-

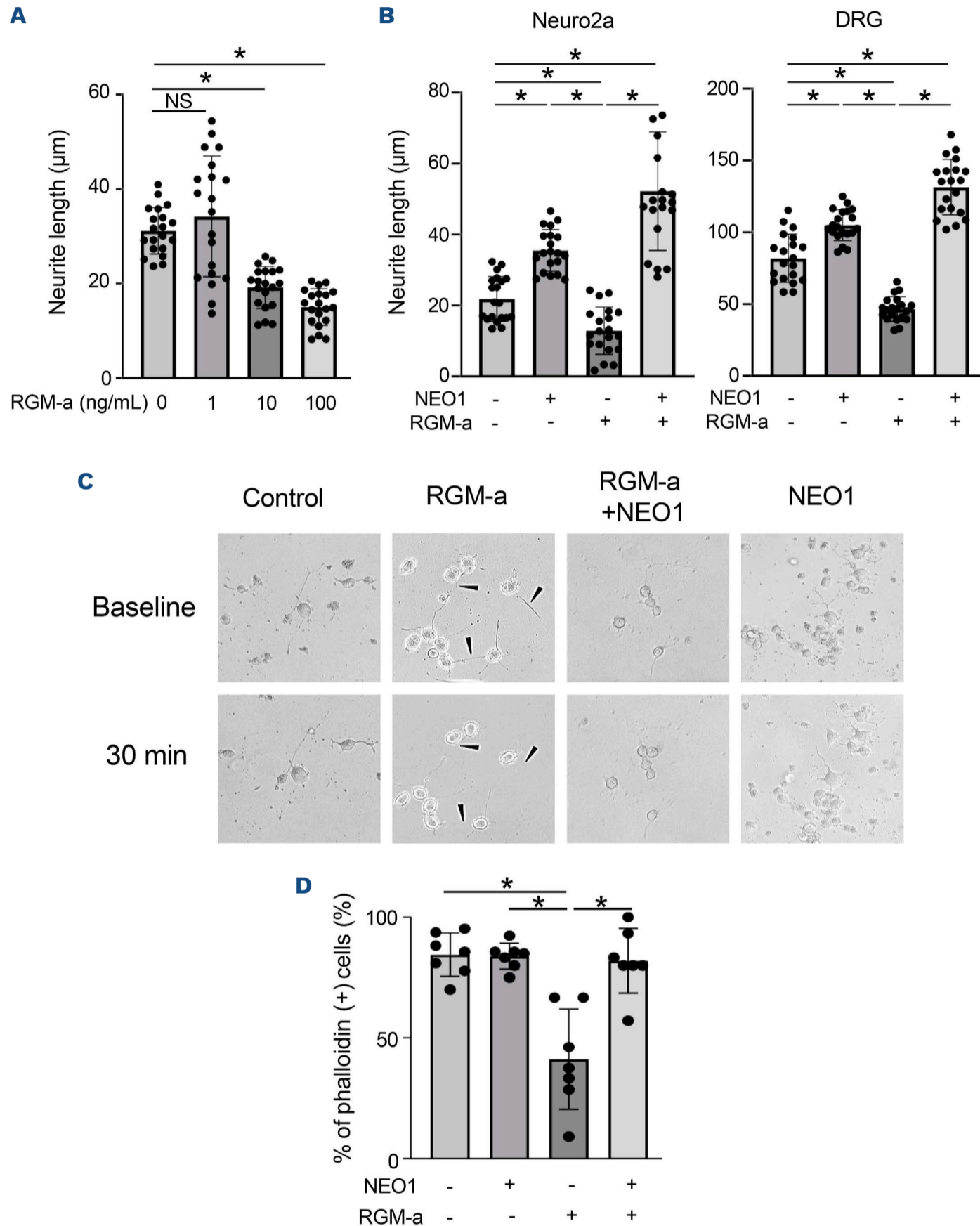


Figure 2. Soluble *NEO1* induces sensory nerve neurite outgrowth through inhibiting *RGM-a*. (A) Recombinant repulsive guidance molecule-a (rRGM-a) was added at the indicated concentrations to Neuro2a in the presence of nerve growth factor (NGF) at 10 ng/mL. After culturing for 2 days, the length of the longest neurite from each cell was measured using NeuronJ. (B) Recombinant neogenin1 (rNEO1) or rRGM-a alone at 100 ng/mL, or both in combination were added to Neuro2a in the presence of NGF at 10 ng/mL and primary dorsal root ganglion (DRG) cells. After culturing for 2 days, the length of the longest neurites from each cell were measured using NeuronJ. Data are expressed as mean \pm standard deviation. * $P < 0.05$. (C) Neuro2a cells were first differentiated into sensory nerves (SN) with extension of their neurites in the presence of NGF at 10 ng/mL. Then, rNEO1 or rRGM-a alone at 100 ng/mL, or both in combination were added as indicated, and neurite retraction was analyzed over time under a phase contrast microscope. The photos were taken at the baseline and after treating for 30 minutes. Arrows indicate retracted neurites. (D) Actin polymerization (F-actin) was detected with phalloidin for the cells treated above in (C). The number of phalloidin-positive cells were counted under a fluorescein microscope (original magnitude, $\times 100$). Data are expressed as mean \pm standard deviation. * $P < 0.05$.

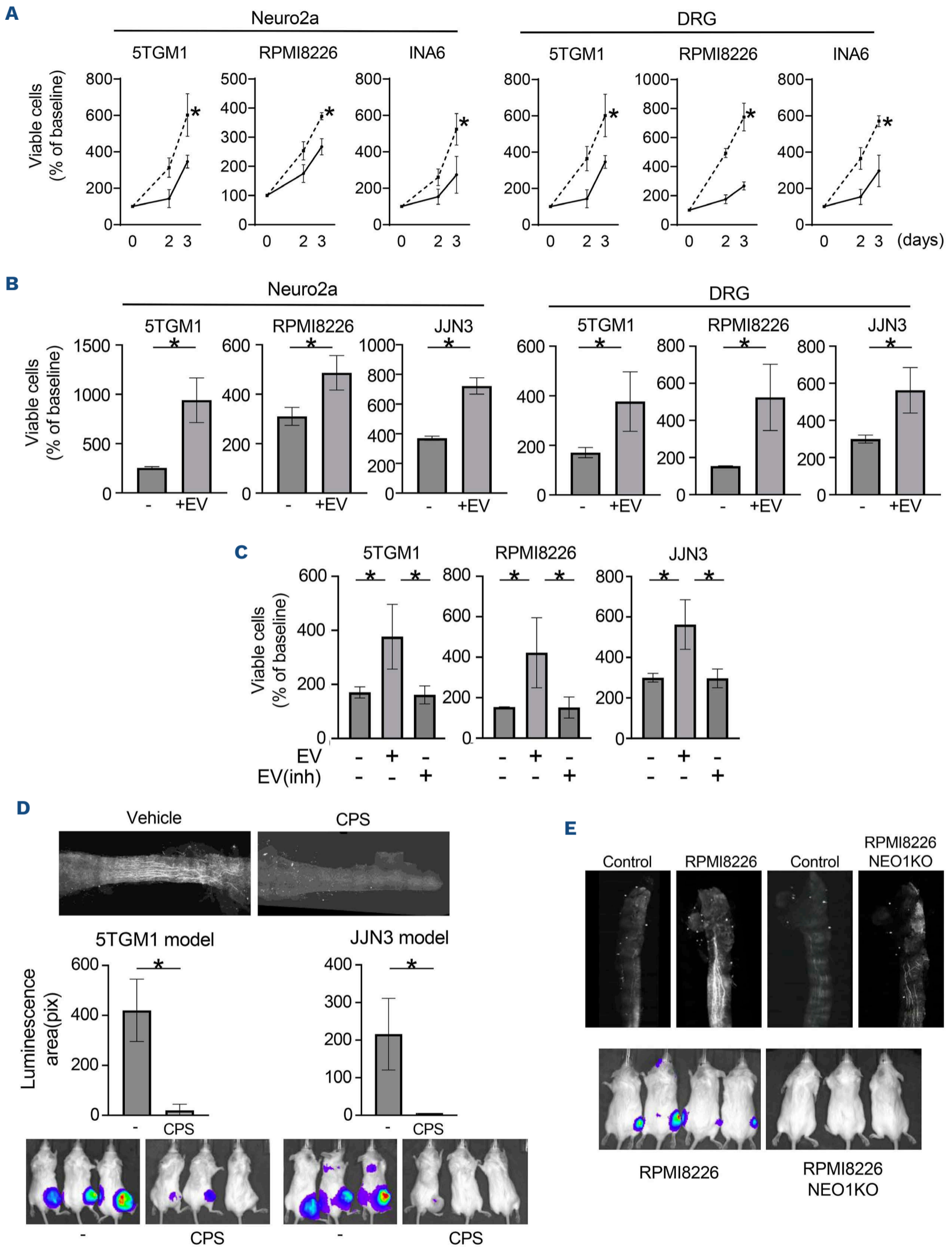


Figure 3. Sensory nerves enhance multiple myeloma cell growth. (A) GFP-expressing multiple myeloma (MM) cell lines were generated by lentiviral transduction with the pLL-CMV-rFLuc-T2A-GFP-mPGK-Puro vector (System Biosciences, Palo Alto, CA, USA). The indicated GFP-expressing MM cell lines were cultured in triplicate at 5×10^4 /mL alone or co-cultured with sensory nerves (SN) derived from the Neuro2a or primary dorsal root ganglia (DRG) cells in 24-well culture plates. The numbers of GFP+MM cells were counted over time under a fluorescence microscope (KEYENCE BZ-X800). (B) Extracellular vesicles (EV) were isolated from

Continued on following page.

culture supernatants of Neuro2a-derived SN and primary DRG cells. EV purification was performed using a material processed with an exosome-affinity component based on sodium polyacrylate, a superabsorbent polymer (SAP) (EXORPTION®, Sanyo Chemical, Kyoto, Japan). After incubation, the SAP was filled into a filter column, then washed 3 times with phosphate-buffered saline (PBS), and PBS was removed at 1,000 rpm for 1 minute (min). The washed SAP was immersed in the extraction solution for 30 min to detach EV from the SAP surface, and EV were collected at 1,000 rpm for 1 min. EV isolated from respective culture supernatants (10 mL) were resuspended in 1 mL (10× concentration). The indicated MM cell lines were cultured at 5.0×10^4 cells/mL in triplicate in culture media with or without the EV. The EV solutions were added to the indicated wells to be diluted 1/10 (approximately 10^9 EV particles/mL). Viable cell numbers were counted at day 3. Percent changes from the baseline were compared. (C) DRG cells were cultured for 2 days in the presence or absence of the miR-21 inhibitor miR-21-IN-3 (MedChemExpress, NJ, USA) at 10 μ M. The cells were washed and cultured in the absence of miR-21-IN-3 for another 2 days to collect culture supernatants for EV isolation. The indicated MM cell lines were cultured at 5×10^4 /mL alone or with EV isolated from the DRG cells pretreated with or without miR-21-IN-3. Values represent the mean \pm standard deviation. * $P < 0.05$. (D) Pharmacological sensory denervation was performed in 4-week-old SCID mice by administering capsaicin (CPS) at a dose of 20 mg/kg body weight or a vehicle (PBS) for 5 consecutive days. Tibiae were resected and subjected to optical clearing with the CUBIC method. CGRP-positive SN were visualized by a light sheet microscope (upper). After the CPS or vehicle treatment, the MM cell lines 5TGM1 and JJN3 transfected with Luc (luciferase) were inoculated into the right tibiae of SCID mice with or without the pharmacological sensory denervation. IVIS images were taken 4 weeks after the inoculation. (E) Neogenin1-knockout (NEO1-KO) or control RPMI8226-Luc cells were inoculated into the right tibiae of SCID mice. Four weeks later, right and left tibiae were resected, and subjected to optical clearing with the CUBIC method. CGRP-positive SN were visualized by a light sheet microscope (upper). IVIS images were taken at 2 weeks after the inoculation (lower). Tumor areas with luminescence were measured. Px: pixels. Data are expressed as mean \pm standard deviation. * $P < 0.05$

motes MM tumor growth to form a vicious cycle between SN hyperplasia and tumor progression in MM. Mechanistically, we found that MM cell-derived soluble NEO1 is a critical mediator for enhancement of sensory innervation in MM. Furthermore, we demonstrated that SN enhance MM cell growth at least in part through SN-secreted EV. SN extend their axons to enhance nociception in acidic conditions in MM bone marrow lesions in mouse models with upregulation of pERK1/2 and pCREB, indicators for neuron excitation, in DRG.¹ Soluble NEO1 further enhanced neurite outgrowth induced in acidic conditions (*Online Supplementary Figure S3F*), suggesting that soluble NEO1 robustly enhances neurite outgrowth in the tumor acidic environment to facilitate the nociception to evoke pain in acidic conditions. Collectively, these results implicate SN as a new niche component in MM, as there has been no previous concept of MM tumor progression being controlled by the peripheral nervous system. Dynamic crosstalk between cancer cells and the peripheral nervous system has been revealed in various types of cancers. MM cells may preferentially reside and colonize in the close vicinity of sensory nerves in bone marrow, which should be deciphered with sophisticated live imaging techniques.

SN distribution is not even in the bone marrow; therefore, it is hard to assess SN density and distribution in the whole bone marrow, using small bone marrow biopsy samples from patients with MM. To address clinical relevance of the present observations, the levels of SN-derived mediators such as CGRP in combination with the levels of soluble NEO1 in bone marrow plasma should be explored in parallel with the development of novel electrophysiological techniques to directly probe SN activity in the bone marrow. Future research will further characterize the neuronal behavior for cell-to-cell interactions with tumor cells as well as microenvironmental cells in MM bone marrow, including vascular, bone and immune cells, besides pain sensation. All procedures involving human samples from healthy do-

nors and patients were performed with written informed consent in accordance with the Declaration of Helsinki and a protocol approved by the Institutional Review Board for human protection at University of Tokushima (permit number 2638-4). This study was also approved by the Genetic Modification Experiment Safety Management Committee of Tokushima University (permit number 2024-10). All animal experiments were conducted under the regulation and permission of the Animal Care and Use Committee of Tokushima University, Tokushima, Japan (permit number T2022-94).

Authors

Motosumi Nakagawa,¹ Masahiro Hiasa,¹ Jumpei Teramachi,² Takeshi Harada,³ Asuka Oda,³ Go Nishino,¹ SooHa Matsuki,¹ Mariko Hanawa,¹ Ariunzaya Bat-Erdene,⁴ Takako Taniguchi,⁵ Hisaaki Taniguchi,⁵ Koichi Tsuneyama,⁶ Tatsuya Tominaga,⁷ Eiji Tanaka,¹ Takeshi Y. Hiyama,⁸ Ken-ichi Matsuoka,³ Yoshio Katayama⁹ and Masahiro Abe¹⁰

¹Department of Orthodontics and Dentofacial Orthopedics, Tokushima University Graduate School of Biomedical Sciences, Tokushima, Japan; ²Department of Oral Function and Anatomy, Faculty of Medicine, Dentistry and Pharmaceutical Sciences, Okayama University Graduate School, Okayama, Japan; ³Department of Hematology, Endocrinology and Metabolism, Tokushima University Graduate School of Biomedical Sciences, Tokushima, Japan; ⁴Department of Immunology, School of Bio-Medicine, Mongolian National University of Medical Sciences; and Department of Health Research, Graduate School of Mongolian National University of Medical Sciences, Ulaanbaatar, Mongolia; ⁵Division of Disease Proteomics, Institute for Enzyme Research, University of Tokushima, Tokushima, Japan; ⁶Department of Pathology and Laboratory Medicine, Tokushima University Graduate School of Biomedical Sciences, Tokushima, Japan; ⁷Department of Bioanalytical Technology, Tokushima University Graduate School of Biomedical Sciences, Tokushima, Japan;

⁸Department of Integrative Physiology, Tottori University Graduate School and Faculty of Medicine, Tottori University, Tottori, Japan; ⁹Hematology, Kobe University Hospital, Kobe, Japan and ¹⁰Department of Hematology, Kawashima Hospital, Tokushima, Japan.

Correspondence:

M. HIASA - mhiasa@tokushima-u.ac.jp

J. TERAMACHI - jumpera@okayama-u.ac.jp

<https://doi.org/10.3324/haematol.2025.300309>

Received: November 27, 2025.

Accepted: February 18, 2026.

Early view: February 26, 2026.

©2026 Ferrata Storti Foundation

Published under a CC BY-NC license 

Disclosures

MA received research funding from Sanofi K.K., and honoraria from Takeda Pharmaceutical, Janssen Pharmaceutical and Daiichi Sankyo Company. The other authors have no conflicts of interest to disclose.

Contributions

MN, MH, TYH, YK, and MA conceived and designed the study. MN,

MH, GN, and MHa performed animal experiments. MN, MH, and GN performed bone specimen clearing and immunostaining. MN, MH, JT, SM, TH, AO, AB, and KM performed cell culture and western blotting. TH, AO, JT, and KT performed immunohistochemical analyses. TH, AO, MH, and JT performed transfection. JT, TTa, and HT performed secretome analyses. MN, JT, SM, and TTo performed EV analyses. MN, MH, JT, TH, TTo, HT, TTa, ET, KM, and MA analyzed data. MN, MH, and MA wrote the manuscript. All authors reviewed and approved the final version of the manuscript.

Funding

This work was supported by AMED-CREST (grant number JP21gm1510001 to TH, TYH, YK, and MA), Grants-in-Aid for Scientific Research (23K27791 and 24K22250 to MH; 24K02643 and 22K19626 to JT) from the Japan Society for the Promotion of Science, and the IMS Career Development Award (2CDA100025 to AB). The funding bodies had no role in the study design, data collection and analysis, decision to publish, or preparation of the manuscript.

Data-sharing statement

Reasonable requests for reagents and data should be addressed to the corresponding authors. Detailed proteomic analyses will be published elsewhere.

References

- Hiasa M, Okui T, Allette YM, et al. Bone pain induced by multiple myeloma is reduced by targeting V-ATPase and ASIC3. *Cancer Res.* 2017;77(6):1283-1295.
- Ji ZZ, Chan MK, Tang PC, et al. Tumor innervation: from bystander to emerging therapeutic target for cancer. *Int J Mol Sci.* 2025;26(18):9257.
- Winkler F, Venkatesh HS, Amit M, et al. Cancer neuroscience: state of the field, emerging directions. *Cell.* 2023;186(8):1689-1707.
- Tainaka K, Murakami TC, Susaki EA, et al. Chemical landscape for tissue clearing based on hydrophilic reagents. *Cell Rep.* 2018;24(8):2196-2210.e2199.
- Thai J, Fuller-Jackson JP, Ivanusic JJ. Using tissue clearing and light sheet fluorescence microscopy for the three-dimensional analysis of sensory and sympathetic nerve endings that innervate bone and dental tissue of mice. *J Comp Neurol.* 2024;532(1):e25582.
- Popko J, Fernandes A, Brites D, Lanier LM. Automated analysis of NeuronJ tracing data. *Cytometry A.* 2009;75(4):371-376.
- Teramachi J, Tenshin H, Hiasa M, et al. TAK1 is a pivotal therapeutic target for tumor progression and bone destruction in myeloma. *Haematologica.* 2021;106(5):1401-1413.
- Wilson NH, Key B. Neogenin: one receptor, many functions. *Int J Biochem Cell Biol.* 2007;39(5):874-878.
- Shimizu M, Shiraishi N, Tada S, et al. RGMa collapses the neuronal actin barrier against disease-implicated protein and exacerbates ALS. *Sci Adv.* 2023;9(47):eadg3193.
- Schreier P, Huang L, Fung E, et al. Development and validation of an ultra-performance liquid chromatography with tandem mass spectrometry method for determination of soluble repulsive guidance molecule A in human serum and cerebrospinal fluid. *Bioanalysis.* 2024;16(21-22):1155-1166.
- Metzger M, Conrad S, Skutella T, Just L. RGMa inhibits neurite outgrowth of neuronal progenitors from murine enteric nervous system via the neogenin receptor in vitro. *J Neurochem.* 2007;103(6):2665-2678.
- Zappulli V, Friis KP, Fitzpatrick Z, Maguire CA, Breakefield XO. Extracellular vesicles and intercellular communication within the nervous system. *J Clin Invest.* 2016;126(4):1198-1207.
- Kim S, Teramachi J, Hiasa M, et al. Myeloma cell growth suppression by osteoblast-derived extracellular vesicles: the creation of a non-permissive niche for myeloma cells by bone-forming osteoblasts. *Haematologica.* 2025;110(6):1395-1401.
- Zhang M, Xian HC, Dai L, Tang YL, Liang XH. MicroRNAs: emerging driver of cancer perineural invasion. *Cell Biosci.* 2021;11(1):117.
- Hu B, Lv X, Chen H, et al. Sensory nerves regulate mesenchymal stromal cell lineage commitment by tuning sympathetic tones. *J Clin Invest.* 2020;130(7):3483-3498.